Autoionization of He and Autodetachment of He⁻ following Bombardment by H^+, H_2^+, He^+, and He Atoms*

F. D. Schowengerdt, S. R. Smart, and M. E. Rudd

Behlen Laboratory of Physics, The University of Nebraska, Lincoln, Nebraska 68508

(Received 10 October 1972)

Presented here are experimental results of a study of the systematics of electron emission from discrete states of He and He⁻ as produced by H^+, H_2^+, He^+, and He impacts. The results were obtained by energy analysis of the electrons emitted at angles of 10° to 160°. Projectile energies ranged from 20 to 150 keV. Differential and integrated cross sections are presented for emission of electrons from the $2s\ ^2(^1S)$, $2s2p(^3P)$, the sum of the $2p\ ^2(^1D)$ and $2s2p(^1P)$ autoionizing levels of He, and the $1s2s\ ^2(^2S)$ autodetaching level of He⁻. The $2s^2(^1S)$ cross section is nearly isotropic, while the $2s2p(^3P)$ and $2p^2(^1D) + 2s2p(^1P)$ cross sections are in general anisotropic. The ratios of the ^3P to the ^1S cross sections follow an approximate $A + B\cos^2\theta$ form. The peak arising from the He⁻ level has an asymmetric profile with a positive q value which increases as the projectile energy decreases.

I. INTRODUCTION

Emission of discrete-energy electrons by helium can occur as a result of autoionization of doubly excited states of the neutral atom or by autodetachment of electrons from the negative ion.

Autoionizing states of neutral helium have been observed in photoabsorption,[1] in inelastic electron scattering,[2-4] and in the energy spectra of electrons emitted following excitation by electrons,[5-8] ions,[9-15] and atoms.[12] In Refs. 7 and 8 studies were made of the electron emission as a function of energy and angle for excitation by electrons, but no detailed study has been made for excitation by ions or neutral atoms.

Excited states corresponding to the temporary formation of He⁻ have been observed as resonances in elastic and inelastic electron scattering.[16-23] Barker and Berry[12] report seeing a peak near 19 eV in the energy distribution of electrons ejected from 4-keV He on He collisions, which they attribute to temporary formation of the $1s2s^2(^2S)$ state of He⁻.

The purpose of the present experiment was to make a systematic study of the emission of electrons from discrete states in He and He⁻ as a function of the type of state involved, the type of projectile used, the projectile energy, and the angle of emission. In this way information can be obtained concerning the excitation and decay mechanisms and kinematic effects. Such information can provide a basis for identifying peaks in other ejected-electron spectra.

For this study, four well-known states in He were chosen, along with a state of He⁻, which had not been observed with heavy projectiles in this energy range. Each of these states requires an excitation mechanism that differs from the others. The $2s2p(^1P)$, for example, can be reached from the ground state by an optically allowed transition,

whereas the $2s^2(^1S)$, $2s2p(^3P)$, and $2p^2(^1D)$ cannot. Of the last three, the $2s2p(^3P)$ can be excited only by electron spin exchange. Excitation of the $1s2s^2(^2S)$ state involves the temporary formation of the negative helium ion through electron exchange with the projectile.

These different excitation mechanisms can be expected to produce different dependences of the emission cross sections on the type and energy of the projectile. The angular dependence, on the other hand, should be a property of the particular state from which the emission occurs and thus independent of the means of excitation. Hence one would expect angular dependences characteristic of the orbital angular momentum of the ejected electron. The extent to which this is true, along with the influence of all of the above factors, will be discussed in the sections that follow.

II. EXPERIMENTAL

Two sets of apparatus were used for the measurements. Both utilized the mass-selected beam from a 150-keV Cockcroft–Walton accelerator.

Measurements of the ejected-electron spectra as a function of angle were made with a parallel-plate electrostatic analyzer which could be positioned at any one of nine fixed ports around the scattering chamber. A detailed description of this apparatus has been published previously,[24,25] so only the essential elements and modifications will be discussed here.

After energy analysis the electrons are detected by an electron multiplier. The amplified output pulses go to a count-rate meter whose output, after being divided by a signal proportional to the beam current, drives the y-axis of an x-y recorder. The x-axis is driven by a linear sweep voltage, which is also applied to the back plate of the analyzer. Details of this analog system are given in Ref. 25. The analog system was used for relative
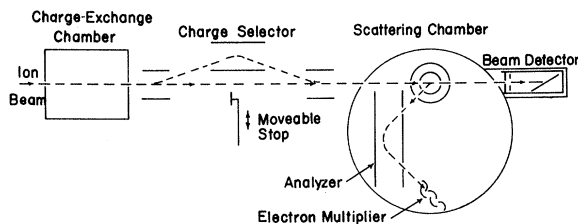
FIG. 1. Schematic diagram of fixed-angle neutral-beam apparatus.

measurements and for quick inspection of the spectra. For absolute-cross-section measurements the output signal was taken directly from the count-rate meter.

Measurements with neutral projectiles were made with the apparatus shown in Fig. 1. Here the ion beam is passed through a charge-exchange chamber filled with a suitable gas. Helium gas was normally used, although adequate neutral beams could be obtained with other gases, including air. The resulting composite beam is then passed through a charge selector where the charged components are removed by electrostatic deflection, or alternatively, the neutral beam is intercepted by a movable stop and the positive or negative component deflected back into the beam path. In principle at least, positive, negative, or neutral projectiles can be produced with this arrangement. However, attempts to produce a He⁻ beam with sufficient intensity to permit ejected-electron measurements were unsuccessful.

The charge-selected beam is then passed into a differentially pumped scattering chamber, where it is collimated to a diameter of 0.33 cm at the scattering center. Biased apertures at the entrance and exit of the chamber serve to suppress secondary electrons. After traversing the collision region the beam is collected in a combination Faraday cup and secondary electron detector.

The beam detector consists of a flat plate of Cu-Be metal set at an angle of 30° relative to the impinging beam and surrounded by a conducting shield. For use as a Faraday cup, the plate and shield are connected together, biased at +67.5 V, and connected through an electrometer to ground. For use as a neutral particle detector, the plate is biased at −67.5 V and connected through an electrometer to ground, while the shield is grounded. Two shielding apertures, the outer grounded and the inner biased at −67.5 V, form the entrance to the detector.

Electrons ejected from the target gas at an angle of 135° relative to the beam pass through a differentially pumped region where they enter a parallel-plate electrostatic analyzer. The analyzer has variable-width entrance and exit slits, but is other-wise similar to the one used on the variable-angle apparatus. After energy analysis the electrons are detected by an electron multiplier. The amplified pulses go to a count-rate meter, which is part of an analog data acquisition system similar to the one described above. All metal parts of the analyzer and all slits through which the electrons pass are gold plated. The back plate of the analyzer is covered with an additional layer of gold deposited in a partial vacuum ("black gold"), which reduces unwanted reflections.

For measurements of the neutral-beam intensity, the secondary emission detector was calibrated as follows: With no gas in the charge-exchange chamber, a He⁺ beam was directed through the system and into the beam detector. With the detector connected as a Faraday cup, a positive ion current I_+ was measured. With the detector connected in the secondary emission mode, a positive current I'_+ was measured. This current is the sum of the positive ion current incident on the plate and the negative secondary electron current leaving the plate. Thus if μ is the secondary emission coefficient of the plate, the ratio R of the two measurements is

$$R = \frac{I'_+}{I_+} = \frac{(\mu+1)I_+}{I_+} ,$$

from which $\mu = R - 1$.

The work of Stier et al.[27] and Wittkower and Gilbody[28] indicates that the secondary emission coefficients for ions and atoms of the rare gases are nearly equal at the energies used here. With this assumption the secondary emission current I'_0 which is measured when the neutral beam strikes the detector is just

$$I'_0 = (R - 1)I_0 ,$$

where I_0 is the neutral atom current. Values of R ranged typically from 7 to 21.

In both sets of apparatus the earth's magnetic field was annulled to less than 10 mG by three mutually perpendicular pairs of 4-ft-diam Helmholtz coils. Target gas pressures were measured with capacitance manometers.

Relative ejected-electron spectra were taken with the fixed-angle apparatus using H⁺, H₂⁺, He⁺, and He projectiles at energies of 20 to 150 keV. Relative spectra were taken with the variable-angle apparatus at eight angles from 10° to 160° using H⁺ and H₂⁺ projectiles at energies of 20 to 120 keV. Absolute data for the eight angles were taken with H⁺ and H₂⁺ at an energy of 100 keV and the relative measurements were normalized to these. The previously measured value of 0.78 was taken for the efficiency of the detector in these measurements.

The uncertainty in the relative measurements of a given spectrum is about 30%, which is repre-
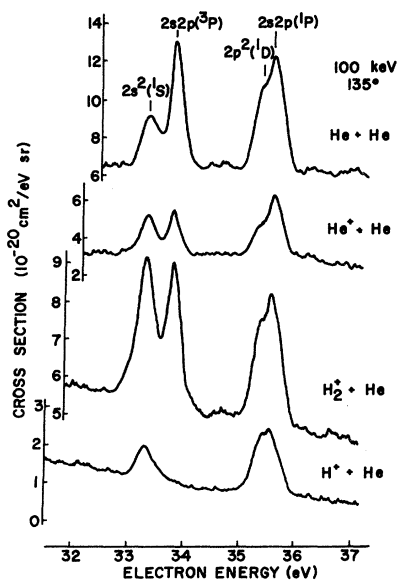
FIG. 2. Ejected-electron spectra in the 30-eV region taken at an ejection angle of 135° and a projectile energy of 100 keV.

sentative of the reproducibility. The uncertainty in the absolute measurements is 50%, which stems primarily from uncertainties in the pressure and detector efficiency measurements.

III. EJECTED-ELECTRON SPECTRA

Samples of the ejected-electron spectra in the 30-eV region for the four different projectiles are shown in Fig. 2. These were taken at an angle of 135° and at a projectile energy of 100 keV. The energy scale was established by taking the energy of the peak resulting from decay of the $2s2p(^1P)$ state to be 35.54 eV. When added to the ionization potential of helium (24.58 eV), this gives the value of 60.12 eV measured spectroscopically by Madden and Codling[1] for the energy of this state. On this scale the peaks from the $2s^2(^1S)$, $2s2p(^3P)$, and $2p^2(^1D)$ levels lie at 33.3, 33.8, and 35.4 eV, respectively, in satisfactory agreement with earlier work in this laboratory[9,10] and with recent electron-impact work.[7,8] The height of the continuum was compared with earlier work in the case of H^+ + He.[24,26] The agreement there is within the combined uncertainties of the three experiments. The resolution was about 1%, which in most cases was not sufficient to completely resolve the $2p^2(^1D)$ and $2s2p(^1P)$ peaks.

The relative effectiveness of the different projectiles in exciting the levels is apparent from Fig. 2. At 100 keV the He projectile appears to be more effective than the He^+ projectile in exciting all the states, as was the case at lower energies. At 150 keV only the ^3P peak showed a strong en-

hancement with the neutral projectiles. At all energies the ^3P peak showed a strong enhancement with He as opposed to He^+ projectiles, with the ratios of the peak heights in the two cases running as high as 3 to 1. Such an effect is to be expected in view of the fact that the ^3P state can be excited only by electron exchange, which is more probable in the He + He case.

In the case of H_2^+ on He all the states are excited more strongly than in the He^+ case, and the ^1S more strongly than in the He case, while the He projectile is more effective in exciting the other states. At an H_2^+ energy of 50 keV, where the velocity is equal to that of the 100-keV He^+ and He projectiles, the H_2^+ excites the ^1S states more by a factor of 2 than does He, but again is less effective in exciting the other states. Thus, although the total number of charges in the H_2^+ projectiles is the same as for He^+, and is less than for He, the effect of the separation of the nuclear charges in H_2^+ is apparently the decisive factor in the excitation of the ^1S state. Excitation of the ^3P state, on the other hand, is not as strong with the H_2^+ projectile as it is with He, owing to the fact that the H_2^+ carries only one electron with which exchange with the target can take place. Finally, the absence of the ^3P peak in the H^+ on He spectrum is consistent with conservation of spin, as has been verified previously in ejected-electron work.[9]

At other angles, greater than 70°, the spectra taken with H^+ and H_2^+ projectiles were similar to those shown in Fig. 2, except for differences in the relative heights of the peaks. However, at angles of 70° and less for H^+, and at 10° for H_2^+, the peaks became asymmetric. With H^+ the asymmetries were present at 70° for high energies and at 10° for all energies. The dependence of the asymmetry on energy and angle has been reported in a recent letter.[29]

Samples of the ejected-electron spectra in the 19-eV region for He on He are shown in Fig. 3. The peak near 19.3 eV results from autodetachment of electrons from the $1s2s^2(^2S)$ state of He^-.

The first experimental evidence for this state was reported by Schulz.[16] He observed a sharp decrease in the electron current elastically scattered from helium at an energy of 19.3 eV and an angle of 72°. Other investigators have verified this work by observing elastically and inelastically scattered electrons.[17-23]

The mechanism for producing the peak here involves electron exchange, with the formation of the compound negative ion state of the target, followed by ejection of a 19.3-eV electron. The peak was not observed with He^+, H_2^+, or H^+. H^+ was not expected to produce the peak, although it did provide a check on the window effect for transmission of electrons through the target gas at the resonance
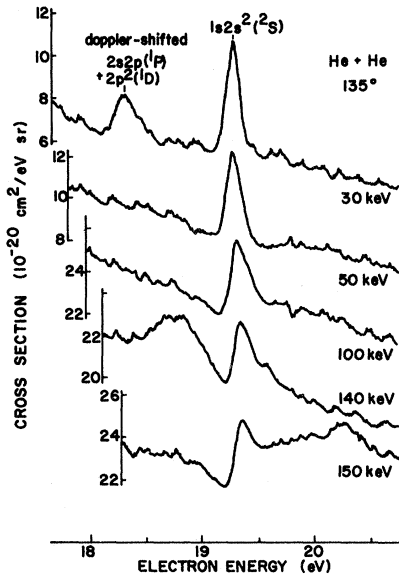
FIG. 3. Ejected-electron spectra in the 19-eV region for He + He, taken at an ejection angle of 135°.

energy. That is, it was conceivable that continuum electrons at 19.3 eV could produce the peak by secondary collisions since they had to pass through some target gas to get to the analyzer, but the effect was not seen. As can be seen in Fig. 3, the shape of the peak varies from symmetrical at the low energies to a pronounced asymmetry at the high energies.

Fano has derived an expression for the shape of

any peak resulting from the coupling of a discrete state and a continuum.[30] According to this derivation the electron-emission cross section $\sigma(\epsilon)$ would be given by

$$\sigma(\epsilon) = \sigma_a + \sigma_b \frac{(q+\epsilon)^2}{1+\epsilon^2}\ ,$$ (1)

where σ_a and σ_b are the nonresonant and resonant cross sections, respectively, $\epsilon = 2(E - E_r)/\Gamma$ is the departure from the resonance energy E_r in units of the resonance half-width $\frac{1}{2}\Gamma$, q is a shape parameter, and E is the electron energy.

Within the limits of our resolution, we can ascertain certain features and trends of the shape parameter q for the data of Fig. 3. The minimum in the cross section given by (1) occurs at $\epsilon = -q$, while the maximum occurs at $\epsilon = 1/q$. The resonance energy E_r lies somewhere in between these two. Therefore, since the minima in the spectra of Fig. 3 occur where ϵ is negative, we conclude that q is positive for the resonance as observed by the present method. This is in agreement with the results of elastic electron scattering experiments at different angles.[16,18] Observations of the resonance in electron transmission experiments[17,22] reveal an asymmetry opposite to that seen here, which is further evidence that the resonance as observed in the present experiment arises from the primary collision rather than from the effect of the transmission window in the target gas.

We note further that as q becomes large the resonance shape approaches a symmetric peak and the location of the peak approaches the true reso-
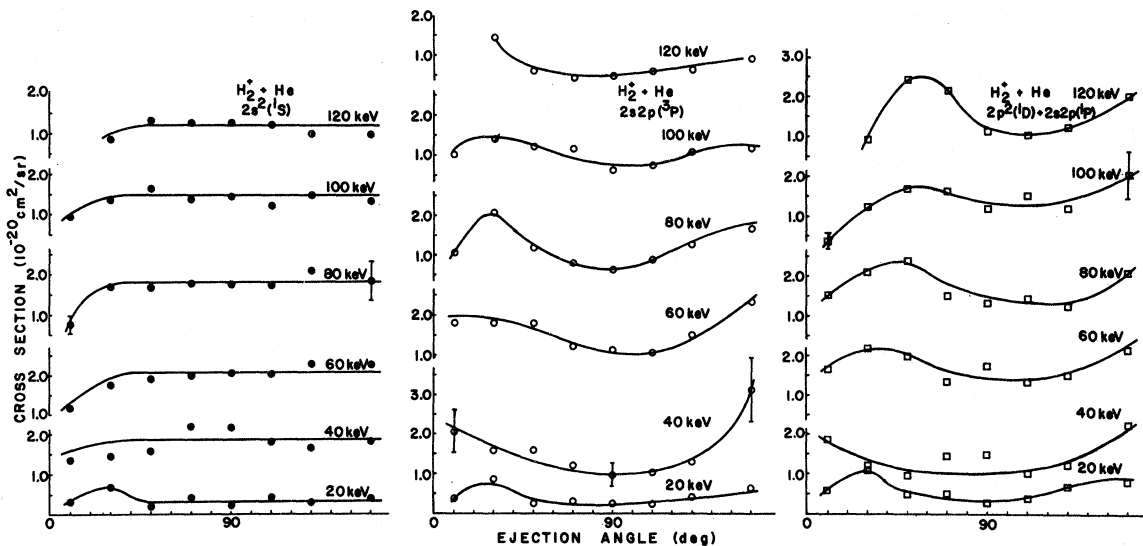

FIG. 4. Integrated cross sections (differential in angle only) for the autoionizing states of He as produced by H_2^+, plotted as a function of ejection angle, with projectile energy as a parameter. Closed circle, $2s^2(^1S)$; open circle, $2s2p(^3P)$; open square, $2p^2(^1D) + 2s2p(^1P)$. The solid lines are possible smooth curves that can be drawn through ±30% error bars. Sample error bars are shown on several of the curves.
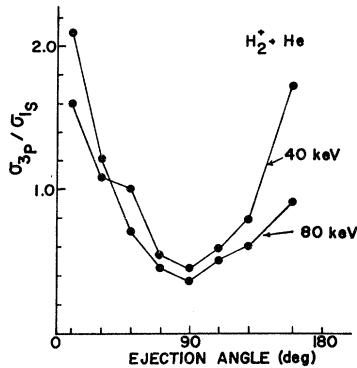
FIG. 5. Ratios of the $2s2p(^3P)$ to the $2s^2(^1S)$ cross section, plotted as a function of ejection angle.

nance energy E_r. Indications of this trend can be seen in the spectra in Fig. 3, where at 150 keV the peak is located at 19.35 eV, decreasing to 19.30 eV at 30 keV.

Two additional features of the He + He spectra in the 10-20 eV region are worth mentioning. First, at energies below 30 keV, doppler-shifted peaks from the autoionizing levels discussed earlier appeared in this region. This effect, first reported by Rudd et al.,[31] results from ejection of electrons from autoionizing states of the projectile. A peak resulting from the $2s2p(^1P)$ and $2p^2(^1D)$ states can be seen in the 30-keV spectrum in Fig. 3. Calculations indicated that the energies and emission angles were consistent with the observed peak locations.

Second, it will be seen from Fig. 3 that there is a broad but pronounced maximum in the continuum in both the 140-keV spectrum and the 150-keV spectrum. The maxima occur at 18.8 and 20.3 eV, respectively, for the two spectra. Electrons with velocities equal to He projectiles with energies of 140 and 150 keV would have energies of 19.1 and 20.4 eV, respectively. This suggests that the broad peak results from elastic scattering of stripped projectile electrons by the target atoms. The number of stripped electrons is a maximum at 0-eV energy in the projectile rest frame, hence the maximum at an electron energy which is velocity equivalent to the projectile in the lab frame. The effect has also been observed by Wilson and Toburen[32] in $H_2^+ + H_2$ collisions at much higher energies. In their work, as in ours, the maxima occur at electron energies which are slightly less than the velocity-equivalent energies.

IV. INTEGRATED CROSS SECTIONS

Electron-emission cross sections for the various states were obtained by integrating under spectra like those shown in Figs. 2 and 3, after subtracting the continuous background. Areas lying above the continuum give a positive contribution to the cross section, while areas lying below give a negative contribution. The integrated cross sections are thus proportional to the excess transition probabilities over and above those for the continua. In terms of the parameters in Eq. (1), the cross sections obtained in this way are of the form

$$\int (\sigma - \sigma_a)dE = \tfrac{1}{2}\Gamma\sigma_b \int \frac{(q+\epsilon)^2}{1+\epsilon^2}\,d\epsilon$$

$$= \tfrac{1}{2}\Gamma\sigma_b(q^2 - 1)\pi,$$

which can be positive or negative, depending on the value of q.

The results for H_2^+ on He are shown in Fig. 4 as a function of angle, with projectile energy as a parameter. Since the ^1P and ^1D peaks could not be separated, their cross sections are shown summed.

With the exception of the points where the peaks were asymmetric, the integrated cross sections for the $2s^2(^1S)$ state are isotropic within the experimental uncertainty. This was true for both H^+ and H_2^+ at all energies. For H_2^+ the effects of the asymmetries were such as to produce decreases in the ^1S cross section of 30% to 70% at 10° as compared to an average value at the other angles.

The integrated cross sections for the $2s2p(^3P)$ state showed an anisotropy which was outside the experimental uncertainty. To eliminate extraneous effects, ratios of the cross sections for the ^3P and ^1S states were taken. These are displayed in Fig. 5 for two representative projective energies. The ratios shown there are of an approximate $A + B\cos^2\theta$ form, where A and B are constants and θ is the ejection angle. The principal departure from this form was a noticeable skewing of the curves toward lower angles with increasing projectile energies and vice versa, a trend which is suggested by the
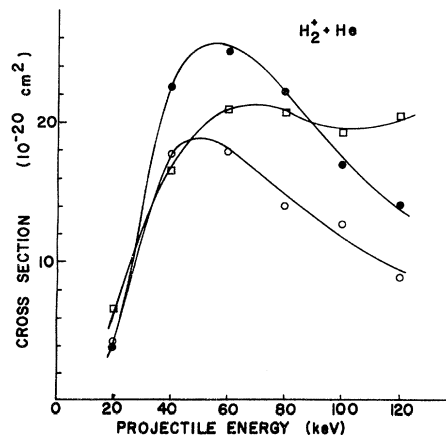

FIG. 6. Total cross sections for the autoionizing states of He as produced by H_2^+. Closed circle, $2s^2(^1S)$; open circle, $2s2p(^3P)$; open square, $2p^2(^1D) + 2s2p(^1P)$.
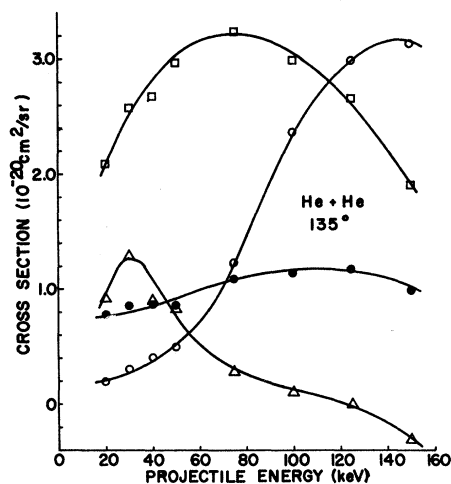
FIG. 7. Integrated cross sections (differential in angle only) for the autoionizing states of He and the autodetaching state of He⁻ as produced by He at 135°. Closed circle, $2s^2(^1S)$; open circle, $2s2p(^3P)$; open square, $2p^2(^1D)$ $+ 2s2p(^1P)$; open triangle, $1s2s^2(^2S)$.

two curves in Fig. 5. Because of this, no attempt was made at a detailed extraction of the parameters A and B for each energy.

Anisotropic angular distributions have been observed by Cleff and Mehlhorn[33] for Auger electrons resulting from $e + Ar$ collisions, and by Gerber et al.[34] for Ar autoionizing electrons from $He + Ar$ collisions. In our case, since the $2s2p(^3P)$ state must decay to the $1s(^2S)$ ground state of He⁺ to produce the observed peak, a p-wave electron must be ejected. Thus the $\cos^2\theta$ distribution results when the beam direction is taken as the axis of quantization.

The integrated cross sections for the sum of the $2s2p(^1P)$ and $2p^2(^1D)$ states also showed an anisotropic distribution (see Fig. 4), but which was not of a simple form as was observed in the ^3P case.

This is undoubtedly due to the fact that we were unable to separate the ^1D component.

Total cross sections for the autoionizing states were obtained from the curves in Fig. 4 by multiplying each point by $2\pi \sin\theta$ and integrating under smooth curves drawn through the resulting points. The results for H_2^+ on He, plotted against projectile energy, are shown in Fig. 6. The optically forbidden nature of the transitions to the ^1S and ^3P states is evident from these curves. The shoulder on the $^1D + ^1P$ curve is probably caused by the forbidden nature of the ^1D transition.

In the He on He case a comparison can be made between excitation of the autoionizing states and the negative ion state. Figure 7 shows the cross sections for He on He at an emission angle of 135°. The cross sections for the autoionizing states show a velocity dependence similar to that found in the H_2^+ on He case, except for the enhancement of the ^3P cross section. In contrast, the cross sections for the $1s2s^2(^2S)$ state of He⁻ show a sharp maximum at a much lower energy and become negative at energies above 120 keV, thus demonstrating the influence of variations in the q value with energy.

V. SUMMARY

The main features of the energy and angular distributions of autoionizing electrons from H_2^+ on He collisions have been established in this work. An anisotropic angular distribution has been observed for the first time in the autoionization of He.

Observation of electrons from the 19.3-eV negative ion state with He bombardment represents a new method for studying this state. By extending the measurements to projectile velocities far below the corresponding threshold for electron excitation, variations of the shape parameters can be studied over a wider range than is possible with electron impact. We are hopeful that other negative ion states will yield to a study by this method.

*Work supported by the National Science Foundation.

[1]R. P. Madden and K. Codling, Astrophys. J. 141, 364 (1965).

[2]J. Arol Simpson, S. R. Mielezarek, and J. Cooper, J. Opt. Soc. Am. 54, 269 (1964).

[3]S. M. Silverman and E. N. Lassettre, J. Chem. Phys. 40, 1265 (1964).

[4]J. Arol Simpson, G. E. Chamberlain, and S. R. Mielczarek, Phys. Rev. 139, A1039 (1965).

[5]W. Mehlhorn, Phys. Lett. 21, 155 (1966).

[6]H. Suzuki, A. Konishi, M. Yamamoto, and K. Wakiya, J. Phys. Soc. Jap. 28, 534 (1970).

[7]N. Oda, F. Nishimura, and S. Tahira, Phys. Rev. Lett. 24, 42 (1970).

[8]G. B. Crooks and M. E. Rudd, in Proceedings of the Seventh International Conference on the Physics of Electronic and Atomic Collisions (North-Holland, Amsterdam, 1971), p. 1035.

[9]M. E. Rudd, Phys. Rev. Lett. 13, 503 (1964); Phys. Rev. Lett. 15, 580 (1965).

[10]M. E. Rudd and D. V. Lang, in Proceedings of the Fourth International Conference on the Physics of Electronic and Atomic Collisions, Quebec 1965, edited by L. Kerwin and W. Fite (Science Bookcrafters, Hastings-on-Hudson, N. Y., 1965), p. 153.

[11]H. W. Berry, Phys. Rev. 121, 1714 (1961).

[12]R. B. Barker and H. W. Berry, Phys. Rev. 151, 14 (1966).

[13]A. Bordenave-Montesquieu, P. Benoit-Cattin, and D. Blanc, in Proceedings of the Seventh International Conference on the Physics of Electronic and Atomic Collisions (North-Holland, Amsterdam, 1971), p. 1041.

[14]A. Bordenave-Montesquieu and P. Benoit-Cattin, Phys. Lett. A 36, 243 (1971).

[15]N. Stolterfoht, Phys. Lett. A 37, 117 (1971).

[16]G. J. Schulz, Phys. Rev. Lett. 10, 104 (1963).

[17]J. Arol Simpson and U. Fano, Phys. Rev. Lett. 11, 158 (1963).

[18]R. J. Fleming and G. S. Higginson, Proc. Phys. Soc. Lond. 81, 974 (1963).

[19]H. Ehrhardt and G. Meister, in Proceedings of the Fourth

International Conference on the Physics of Electronic and Atomic Collisions, Quebec 1965, edited by L. Kerwin and W. Fite (Science Bookcrafters, Hastings-on-Hudson, N. Y., 1965), p. 125.

[20]G. J. Schulz and J. W. Philbrick, Phys. Rev. Lett. **13,** 477 (1964).

[21]G. E. Chamberlain, Phys. Rev. Lett. **14,** 581 (1965).

[22]C. E. Kuyatt, J. Arol Simpson, and S. R. Mielczarek, Phys. Rev. **138,** A385 (1965).

[23]G. J. Schulz, in *Proceedings of the Fourth International Conference of the Physics of Electronic and Atomic Collisions, Quebec, 1965* (Science Bookcrafters, Hastings-on-Hudson, N. Y., 1965), p. 117.

[24]M. E. Rudd and T. Jorgensen, Jr., Phys. Rev. **131,** 666 (1963).

[25]M. E. Rudd, Rev. Sci. Instrum. **37,** 971 (1966).

[26]M. E. Rudd, C. A. Sautter, and C. L. Bailey, Phys. Rev. **151,** 20 (1966).

[27]P. M. Stier, C. F. Barnett, and G. E. Evans, Phys. Rev. **96,** 973 (1954).

[28]A. B. Wittkower and H. B. Gilbody, Proc. Phys. Soc. Lond. **90,** 353 (1967).

[29]F. D. Schowengerdt and M. E. Rudd, Phys. Rev. Lett. **28,** 127 (1971).

[30]U. Fano, Phys. Rev. **124,** 1866 (1961).

[31]M. E. Rudd, T. Jorgensen, Jr., and D. J. Volz, Phys. Rev. Lett. **16,** 929 (1966).

[32]W. E. Wilson and L. H. Toburen (private communication).

[33]B. Cleff and W. Mehlhorn, Phys. Lett. A **37,** 3 (1971).

[34]G. Gerber, R. Morgenstern, A. Niehaus, and M. W. Ruf, in *Proceedings of the Seventh International Conference on the Physics of Electronic and Atomic Collisions* (North-Holland, Amsterdam, 1971), p. 610.

Gold L X-Ray Production by 0.5–30-MeV Protons*

S. M. Shafroth and G. A. Bissinger†

University of North Carolina, Chapel Hill, North Carolina 27514

Triangle Universities Nuclear Laboratory, Durham, North Carolina 27706

and

A. W. Waltner

North Carolina State University, Raleigh, North Carolina 27607

Triangle Universities Nuclear Laboratory, Durham, North Carolina 27706

(Received 21 July 1972)

The characteristic L x-rays of Au, produced by 0.5–30-MeV proton beams on a thin Au target have been observed with a Si(Li) detector. Total L x-ray production cross sections derived from these measurements are in good agreement with presently available theoretical calculations. However, theoretical predictions of $L\alpha/L\beta$ and $L\alpha/L\gamma$ ratios and centroid energies of the $L\beta$ and $L\gamma$ lines as functions of proton energy show that a consistent quantum-mechanical treatment of L-shell ionization gives considerably better agreement with experimental results than the semiclassical or classical theories of inner-shell ionization.

I. INTRODUCTION

There is extensive experimental work on K-shell ionization by protons ranging in energy from 20 keV to 160 MeV over the whole Periodic Table. In general, the plane-wave Born approximation (PWBA), presented most completely by Merzbacher and Lewis,[1] which uses nonrelativistic hydrogenic wave functions, predicts K-shell ionization cross sections σ_K that are in good agreement with experimental values for σ_K at proton energies considerably above the binding energy. At lower proton energies the PWBA results usually lie above the experimental values of σ_K. This is considered to be due to nuclear repulsion effects. Bang and Hansteen[2] have treated the repulsion effects in a semiclassical approximation (SCA) by allowing the incoming projectile to follow a classical hyperbolic trajectory, which permits an impact-parameter description of the ionization process, while still providing a quantum-mechanical treatment of the atom. The SCA theory gives improved agreement with experimental measurements of σ_K at low projectile energies. Recently, a classical binary-encounter (BEA) description of K-shell ionization has been proposed by Garcia,[3] which includes nuclear repulsion effects. This is observed to give good agreement with experimental results over a broad proton energy range.[4] The experimental cross sections are generally derived from x-ray yield measurements, which required correction for the fluorescence yield. Presently there are reliable values[5] of ω_K for $Z \geq 10$, while for $Z < 10$, the situation is not nearly so clear.

The experimental measurements of L-shell ionization cross sections σ_L are not nearly so extensive, most measurements being for high-Z elements with low-energy protons (< 4 MeV). Recent measurements[6] with 2–30-MeV protons on Ag indicated that experimental values for σ_L fell consistently higher than either PWBA or BEA predictions (possibly because of inaccuracy in the value of the mean fluorescence yield $\bar{\omega}_L$ used to compare the L x-ray production cross section σ_{LX} with theoretical values of σ_L), although the observed energy dependence of σ_L was in better